

# INELASTIC LIGHT SCATTERING AND THE CORRELATED METAL-INSULATOR TRANSITION

J.K. FREERICKS ([freericks@physics.georgetown.edu](mailto:freericks@physics.georgetown.edu))  
*Department of Physics, Georgetown University, Washington,  
DC 20057, U.S.A.*

T.P. DEVEREAUX ([tpd@lorax.uwaterloo.edu](mailto:tpd@lorax.uwaterloo.edu))  
*Department of Physics, University of Waterloo, Canada*

R. BULLA ([ralf.bulla@physik.uni-augsburg.de](mailto:ralf.bulla@physik.uni-augsburg.de))  
*Theoretische Physik III, Elektronische Korrelationen und Magnetismus, Institut für Physik, Universität Augsburg, D-86135, Augsburg, Germany*

Abstract. Inelastic light scattering is an important probe of the two-particle charge excitations in a correlated material. We show how to determine the nonresonant response to inelastic light scattering exactly in the limit of large spatial dimensions by employing dynamical mean field theory. We examine the optical photon case of Raman scattering and the X-ray photon scattering case which exchanges both energy and momentum with the charge excitations. A number of formal details that have not appeared elsewhere are included here.

## 1. Introduction

In correlated materials, two-particle properties, such as charge fluctuations, may be quite different from single-particle properties (such as the interacting density of states measured in photoemission). In particular, one expects significant renormalization effects of the charge excitations near the correlated metal-insulator transition. There are a number of direct experimental probes of the charge excitations in a material. The most common probe is an optical conductivity measurement, which is either performed directly in a transmission geometry in the THz range, or involves a Kramers-Kronig analysis of reflectivity data for higher frequencies. Another important experimental probe involves the inelastic scattering of light from the charge excitations. If optical photons are used, the process is called electronic Raman scattering, and only energy is exchanged with the correlated charge

excitations. If X-rays are employed, then both energy and momentum are exchanged with the charge excitations.

The theoretical description of inelastic light scattering is complicated, and has only been solved recently in the limit of large dimensions (1, 2, 3). This solution involves the exact evaluation of the two-particle diagrams for nonresonant inelastic light scattering. Nonresonant scattering implies that there is no feedback effect from the energy of the incident photon, and only the transferred photon energy (and momentum) enters into the scattering response function. While it is well known that many resonant scattering effects exist, and indeed, resonant effects are necessary for some experiments to even be possible, the main qualitative features of the inelastic scattering process are contained in the nonresonant formalism. Furthermore, the computations are significantly more tractable.

## 2. Formal Development

We employ dynamical mean-field theory (DMFT) to solve the inelastic light scattering problem. In DMFT, the electronic self energy is local, and only the local piece of the irreducible vertex function enters into any physical response function. We describe below how to formulate the inelastic light scattering problem on a hypercubic lattice in  $d \rightarrow \infty$  dimensions. It turns out that much of the formalism is independent of the explicit form of the Hamiltonian, but the interactions must all be local. For concreteness, we consider the Hubbard Hamiltonian (4)

$$\mathcal{H} = -\frac{t^*}{2\sqrt{d}} \sum_{\langle i,j \rangle, \sigma} (c_{i\sigma}^\dagger c_{j\sigma} + c_{j\sigma}^\dagger c_{i\sigma}) + U \sum_i c_{i\uparrow}^\dagger c_{i\uparrow} c_{i\downarrow}^\dagger c_{i\downarrow}, \quad (1)$$

with rescaled hopping integral  $t^*$  (5) (between nearest neighbors—the summation is over nearest-neighbor pairs) and screened Coulomb integral  $U$ . The  $c_{i\sigma}^\dagger$  ( $c_{i\sigma}$ ) operators create (destroy) an electron with spin  $\sigma$  at site  $i$ . The noninteracting bandstructure is  $\epsilon(\mathbf{k}) = -\lim_{d \rightarrow \infty} \sum_{i=1}^d t^* \cos(k_i) / \sqrt{d}$  and the noninteracting DOS becomes  $\rho(\epsilon) = \exp(-\epsilon^2) / t^* \sqrt{\pi}$ . The inelastic light scattering response function is given by an effective density-density correlation function  $S(\mathbf{q}, \nu) = -\frac{1}{\pi} [1 + n(\nu)] \text{Im} \chi(\mathbf{q}, \nu)$  for transferred momentum  $\mathbf{q}$  and energy  $\nu$  with

$$\chi(\mathbf{q}, \nu) = \langle [\tilde{\rho}(\mathbf{q}), \tilde{\rho}(-\mathbf{q})] \rangle_{(\nu)} \quad (2)$$

formed with an “effective” density operator given by

$$\tilde{\rho}(\mathbf{q}) = \sum_{\mathbf{k}, \sigma} \gamma_a(\mathbf{k}) c_\sigma^\dagger(\mathbf{k} + \mathbf{q}/2) c_\sigma(\mathbf{k} - \mathbf{q}/2), \quad (3)$$

where the  $c_\sigma^\dagger(\mathbf{k})$  and  $c_\sigma(\mathbf{k})$  operators create or destroy an electron with spin  $\sigma$  and momentum  $\mathbf{k}$  and  $n(\nu) = 1/[1 - \exp(\nu/T)]$  is the Bose factor. The strength of the scattering  $\gamma_a$  is determined by the curvature of the band as

$$\gamma_a(\mathbf{k}) = \sum_{\alpha,\beta} e_\alpha^s \frac{\partial^2 \epsilon_{\mathbf{k}}}{\partial k_\alpha \partial k_\beta} e_\beta^i. \quad (4)$$

Here  $\mathbf{e}^{i,s}$  denote the incident, scattered photon polarization vectors, respectively, and we have chosen units  $k_B = c = \hbar = t^* = 1$  and have set the hypercubic lattice constant equal to 1. We can classify the scattering amplitudes by point group symmetry operations. If we choose  $\mathbf{e}^i = (1, 1, 1, \dots)$  and  $\mathbf{e}^s = (1, -1, 1, -1, \dots)$ , then we have the  $B_{1g}$  sector, while  $\mathbf{e}^i = \mathbf{e}^s = (1, 1, 1, \dots)$  projects out the  $A_{1g}$  sector since the  $B_{2g}$  component is identically zero in our model due to the inclusion of only nearest-neighbor hopping (1). Hence  $\gamma_{A_{1g}}(\mathbf{q}) = -\epsilon(\mathbf{q})$  and  $\gamma_{B_{1g}}(\mathbf{q}) = t^* \sum_{j=1}^{\infty} \cos \mathbf{q}_j (-1)^j / \sqrt{d}$ .

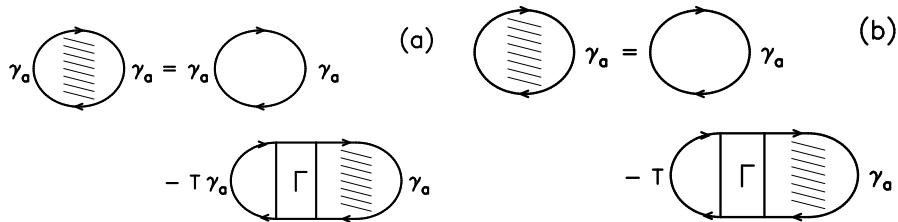


*Figure 1.* Coupled Dyson equations for the inelastic light scattering density-density correlation functions described by the scattering amplitude  $\gamma_a$ . Panel (a) depicts the Dyson equation for the interacting correlation function, while panel (b) is the supplemental equation needed to solve for the correlation function (the difference in the two equations is the number of  $\gamma_a$  factors). The symbol  $\Gamma$  stands for the local dynamical irreducible charge vertex. In situations where there are no charge vertex corrections (like  $B_{1g}$  scattering along the zone-diagonal), the correlation function is simply given by the first (bare-bubble) diagram on the right hand side of panel (a).

The Dyson equation for the density-density correlation function takes the form given in Figure 1. Note that there are two coupled equations illustrated in Figures 1 (a) and (b); these equations differ by the number of  $\gamma_a$  factors in them. The irreducible vertex function  $\Gamma$  is the dynamical charge vertex which is known explicitly only for the Falicov-Kimball model (6). If the scattering amplitude  $\gamma$  does not have a projection onto the full symmetry of the lattice, then there are no vertex corrections from the local dynamical charge vertex (7). This is the only case that can be analyzed for the Hubbard model.

Let's begin our discussion on the imaginary axis in the  $B_{1g}$  sector. If we restrict ourselves to the zone diagonal, then  $\mathbf{q} = (q, q, q, \dots, q)$ . Examining

the diagrams in Figure 1 (a), we see that there is a bare response plus a vertex correction term. The vertex correction term, however, must vanish, because the leftmost piece of that diagram is

$$0 = -T \sum_n \sum_{\mathbf{k}} \lim_{d \rightarrow \infty} \sum_{j=1}^d \frac{\cos(k_j)(-1)^j}{\sqrt{d}} \frac{1}{i\omega_n + \mu - \Sigma(i\omega_n) - \epsilon(\mathbf{k} - \frac{1}{2}\mathbf{q})} \\ \times \frac{1}{i\omega_n + i\nu_l + \mu - \Sigma(i\omega_n + i\nu_l) - \epsilon(\mathbf{k} + \frac{1}{2}\mathbf{q})} \quad (5)$$

for “energy” transfer  $i\nu_l = 2i\pi Tl$  and momentum transfer  $\mathbf{q}$  [in Eq. (5)  $i\omega_n = i\pi T(2n + 1)$  is the fermionic Matsubara frequency and  $\mu$  is the chemical potential]. It vanishes, because each term indexed by  $j$  is equal in magnitude, but opposite in sign, so the overall summation is equal to zero. Hence the  $B_{1g}$  response on the zone diagonal (including the Raman response) is given by the bare bubble.

The bare bubble on the zone diagonal is simple to calculate directly (we shift  $\mathbf{k} \rightarrow \mathbf{k} + \mathbf{q}/2$ ):

$$\chi_0(\mathbf{q}, i\nu_l) = -T \sum_n \sum_{\mathbf{k}} \lim_{d \rightarrow \infty} \sum_{i,j=1}^d \frac{\cos(k_i + \frac{1}{2}q) \cos(k_j + \frac{1}{2}q)(-1)^{i+j}}{d} \\ \times \frac{1}{i\omega_n + \mu - \Sigma(i\omega_n) - \epsilon(\mathbf{k})} \\ \times \frac{1}{i\omega_n + i\nu_l + \mu - \Sigma(i\omega_n + i\nu_l) - \epsilon(\mathbf{k} + \mathbf{q})}. \quad (6)$$

Now, the terms with  $i \neq j$  are all equal in magnitude, but there are as many positive as negative, so they vanish—only the terms with  $i = j$  survive. If we assume that  $n$  and  $n + l$  are both larger than 0, and define  $Z_n = i\omega_n + \mu - \Sigma(i\omega_n)$ , then we can rewrite the fractions as integrals of exponentials

$$\chi_0(\mathbf{q}, i\nu_l) = T \sum_n \sum_{\mathbf{k}} \lim_{d \rightarrow \infty} \sum_{j=1}^d \frac{\cos^2(k_j + \frac{1}{2}q)}{d} \\ \times \int_0^\infty d\lambda \int_0^\infty d\lambda' \exp[i\lambda Z_n + i\lambda' Z_{n+l} - i\lambda\epsilon(\mathbf{k}) - i\lambda'\epsilon(\mathbf{k} + \mathbf{q})]. \quad (7)$$

To evaluate this integral, we first expand the functions  $\epsilon(\mathbf{k})$  and  $\epsilon(\mathbf{k} + \mathbf{q})$  in terms of the Cartesian momentum components. Then it is obvious that each  $j$  term is equal in magnitude, so the sum over  $j$  is trivial. The next step is to expand each exponential factor that has a  $1/\sqrt{d}$  prefactor in a Taylor series expansion, and keep the lowest nonvanishing terms in the multiple integrals (8). The multiple integral over momentum then becomes

$$\lim_{d \rightarrow \infty} \int dk_1 \int dk_2 \dots \int dk_d \cos^2(k_1 + \frac{q}{2})$$

$$\prod_{j=1}^d \left( 1 + \frac{i}{\sqrt{d}} \lambda \cos k_j + \frac{i}{\sqrt{d}} \lambda \cos(k_j + q) - \frac{\lambda^2}{2d} \cos^2 k_j - \frac{\lambda \lambda'}{d} \cos k_j \cos(k_j + q) - \frac{\lambda'^2}{2d} \cos^2(k_j + q) + \dots \right). \quad (8)$$

Here we have chosen the extra prefactor to lie in the 1 direction. Each integral over  $k_j$ , except the first, is equal to each other and equal to  $1 - (\lambda^2 + 2\lambda\lambda'X(\mathbf{q}) + \lambda'^2)/4d + \dots$ . The first integral becomes  $\frac{1}{2}[1 - (\lambda^2 + 2\lambda\lambda'X(\mathbf{q}) + \lambda'^2)/4d - (\lambda\lambda' + \lambda'^2 \cos q) \sin^2 q/8d + \dots]$ . Here we use the notation  $X(\mathbf{q}) = \lim_{d \rightarrow \infty} \sum_{j=1}^d \cos q_j/d$  ( $= \cos q$  for a zone-diagonal momentum). The next step is to rewrite each factor as an exponential, and then take the infinite product. The result for the integral over  $\mathbf{k}$  is

$$\frac{1}{2} \exp \left[ -\frac{\lambda^2 + 2\lambda\lambda'X(\mathbf{q}) + \lambda'^2}{4} \right] \quad (9)$$

since the terms proportional to  $\sin^2 q$  coming from the 1-direction are just a  $1/d$  correction. The end result for the susceptibility is then

$$\chi_0(\mathbf{q}, i\nu_l) = -\frac{1}{2} \int d\epsilon \rho(\epsilon) \frac{1}{Z_n - \epsilon} \frac{1}{\sqrt{1 - X^2}} F_\infty \left( \frac{Z_{n+l} - X\epsilon}{\sqrt{1 - X^2}} \right), \quad (10)$$

with  $F_\infty$  the Hilbert transformation of the DOS:  $F_\infty(z) = \int d\epsilon \rho(\epsilon)/(z - \epsilon)$ .

The analytic continuation of this expression is straightforward, and produces the final result for the  $B_{1g}$  response

$$\begin{aligned} \chi_{B_{1g}}(\mathbf{q}, \nu) &= \frac{i}{4\pi} \int_{-\infty}^{\infty} d\omega \{ f(\omega) \chi_0(\omega; X, \nu) - f(\omega + \nu) \chi_0^*(\omega; X, \nu) \\ &\quad - [f(\omega) - f(\omega + \nu)] \tilde{\chi}_0(\omega; X, \nu) \} \end{aligned} \quad (11)$$

with

$$\begin{aligned} \chi_0(\omega; X, \nu) &= - \int_{-\infty}^{\infty} d\epsilon \rho(\epsilon) \frac{1}{\omega + \mu - \Sigma(\omega) - \epsilon} \frac{1}{\sqrt{1 - X^2}} \\ &\quad \times F_\infty \left( \frac{\omega + \nu + \mu - \Sigma(\omega + \nu) - X\epsilon}{\sqrt{1 - X^2}} \right), \end{aligned} \quad (12)$$

and

$$\begin{aligned} \tilde{\chi}_0(\omega; X, \nu) &= - \int_{-\infty}^{\infty} d\epsilon \rho(\epsilon) \frac{1}{\omega + \mu - \Sigma^*(\omega) - \epsilon} \frac{1}{\sqrt{1 - X^2}} \\ &\quad \times F_\infty \left( \frac{\omega + \nu + \mu - \Sigma(\omega + \nu) - X\epsilon}{\sqrt{1 - X^2}} \right). \end{aligned} \quad (13)$$

Here  $f(\omega) = 1/[1 + \exp(\omega/T)]$  is the fermi factor.

A similar, but more complicated analysis can be performed for the  $A_{1g}$  response, or the  $B_{1g}$  response off of the zone diagonal, but we don't have enough space to report those results here, and they cannot be analyzed numerically for the Hubbard model.

### 3. Results

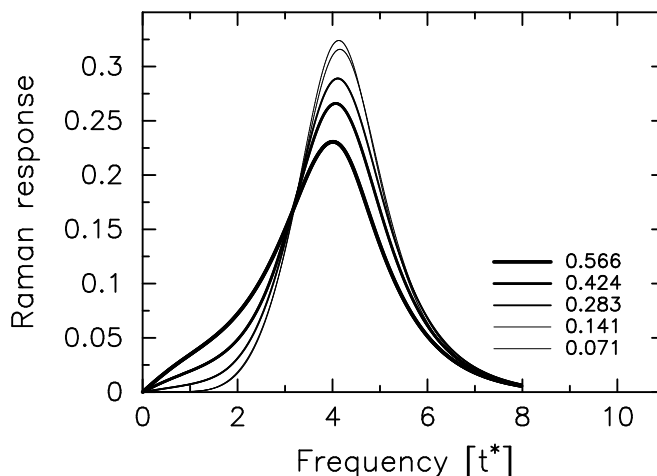


*Figure 2.* Nonresonant  $B_{1g}$  Raman response ( $X = 1$ ) for different temperatures at  $U = 4.24$  and half filling. The numbers in the legends label the temperature.

We employ a numerical renormalization group analysis to determine the self energy and Green's function of the Hubbard model on the real axis (9). We begin by showing Raman scattering results at half filling for  $U = 4.24$  and a variety of temperatures in Figure 2. At this value of  $U$ , the system is a correlated insulator for all temperatures. The results display all of the behavior seen on correlated insulators like FeSi (10), or SmB<sub>6</sub> (11), or the high-temperature superconductors (12). In particular, we see a charge-transfer peak at high-energy and the onset of low-energy spectral weight at a low (but nonzero) temperature. The curves also cross at the so-called isosbestic point (near  $\nu \approx 3.2$ ).

We show the inelastic X-ray scattering at four different temperatures for a slightly smaller value of  $U$  and at  $n = 0.9$  in Figure 3. Here the behavior is quite different because the system is metallic for all temperatures. In particular, we see a Fermi-liquid peak form and evolve toward zero frequency as  $T$  is lowered for momentum transfer near the zone diagonal. But for finite momentum transfer, the peak never fully evolves. In addition,

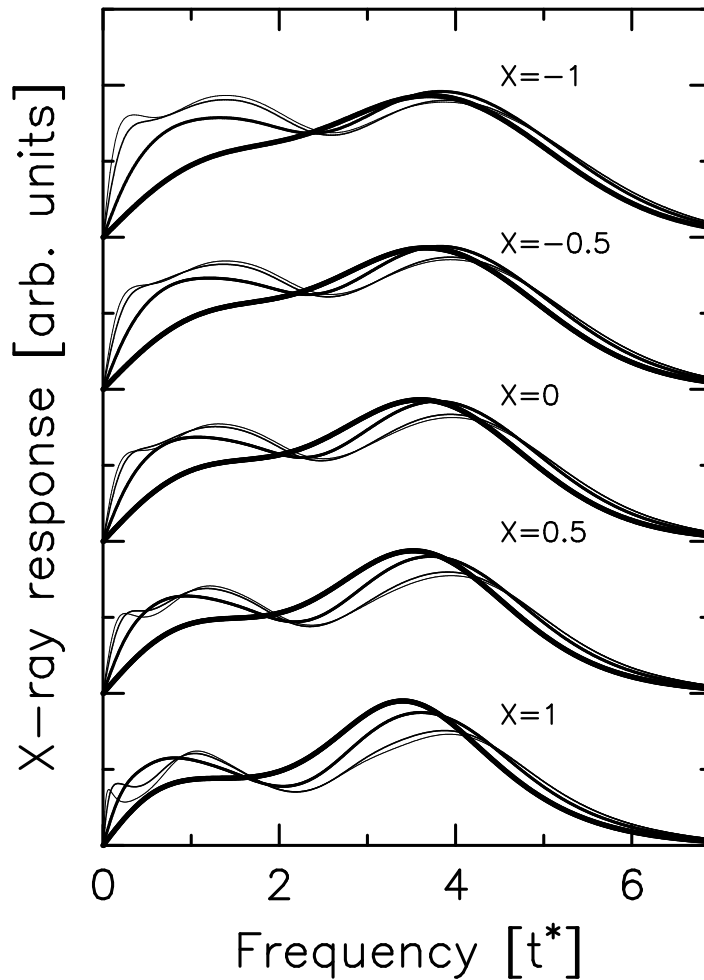


*Figure 3.* Nonresonant  $B_{1g}$  inelastic X-ray response for different temperatures at  $U = 3.54$  and  $\rho_e = 0.9$ . Five values of the transferred photon momentum are plotted, each shifted by an appropriate amount, and running from the zone center ( $X = 1$ ) to the zone boundary ( $X = -1$ ) along the zone diagonal. The temperature decreases with decreasing thickness of the lines and ranges from 0.503 to 0.114 to 0.042 to 0.026.

there is significant “mid-IR” spectral weight occurring at energies below the charge-transfer peak but not corresponding to the fermi peak.

#### 4. Conclusions

We have presented a number of new results for the inelastic scattering of light with correlated materials. On the insulating side of the metal-

insulator transition, Raman scattering results agree well with experiments that have been performed on a wide variety of different materials. We find a number of interesting features for correlated metals as well, and it would be interesting to experimentally measure both Raman scattering and inelastic X-ray scattering for these materials. We expect this behavior might be able to be seen in a variety of different heavy-fermion compounds.

### Acknowledgements

J.K.F. acknowledges support of the National Science Foundation under grants DMR-9973225 and DMR-0210717. T.P.D. acknowledges support from the National Research Council of Canada. R.B. acknowledges support by the Deutsche Forschungsgemeinschaft, through Sonderforschungsbereich 484.

### References

1. J.K. Freericks and T.P. Devereaux, *J. Cond. Phys. (Ukraine)* **4**, 149 (2001); *Phys. Rev. B* **64**, 125110 (2001).
2. J.K. Freericks, T.P. Devereaux, and R. Bulla, *Acta Phys. Pol. B* **32**, 3219 (2001); *Phys. Rev. B* **64**, 233114 (2001); unpublished.
3. T.P. Devereaux, G. E. D. McCormack, and J.K. Freericks, *submitted to Phys. Rev. Lett.* (cond-mat/0208049).
4. J.C. Hubbard, *Proc. Royal Soc. London, Ser. A* **276**, 238 (1963).
5. W. Metzner and D. Vollhardt, *Phys. Rev. Lett.* **62**, 324 (1989).
6. A. M. Shvaika, *Physica C* **341–348**, 177 (2000); J. K. Freericks and P. Miller, *Phys. Rev. B* **62**, 10022 (2000); A. M. Shvaika, *J. Phys. Stud.* **5**, 349 (2002).
7. A. Khurana, *Phys. Rev. Lett.*, **64**, 1990 (1990).
8. E. Müller-Hartmann, *Int. J. Phys. B* **3**, 2169 (1989).
9. R. Bulla, *Phys. Rev. Lett.* **83**, 136 (1999); R. Bulla, T. A. Costi, and D. Vollhardt, *Phys. Rev. B* **64**, 045103 (2001).
10. P. Nyhus, S.L. Cooper, and Z. Fisk, *Phys. Rev. B* **51**, R15626 (1995).
11. P. Nyhus, S.L. Cooper, Z. Fisk, and J. Sarrao, *Phys. Rev. B* **52**, R14308 (1995); *Phys. Rev. B* **55**, 12488 (1997).
12. X. K. Chen, J.G. Naeni, K.C. Hewitt, J.C. Irwin, R. Liang, W.N. Hardy, *Phys. Rev. B* **56**, R513 (1997); J.G. Naeni, X.K. Chen, J.C. Irwin, M. Okuya, T. Kimura, and K. Kishio, *Phys. Rev. B* **59**, 9642 (1999); M. Rübhausen, O.A. Hammerstein, A. Bock, U. Merkt, C.T. Rieck, P. Guptasarma, D.G. Hinks, M.V. Klein, *Phys. Rev. Lett.* **82**, 5349 (1999); S. Sugai and T. Hosokawa, *Phys. Rev. Lett.* **95**, 1112 (2000); M. Opel, R. Nemeschek, C. Hoffmann, R. Philipp, P.F. Müller, R. Hackl, I. Tüttö, A. Erb, B. Revaz, E. Walker, H. Berger, and L. Forró, *Phys. Rev. B* **61**, 9752 (2000); F. Venturini, M. Opel, T. P. Devereaux, J. K. Freericks, I. Tüttö, B. Revaz, E. Walker, H. Berger, L. Forró and R. Hackl, *Phys. Rev. Lett.* **89**, 107003 (2002).